



Regulation of Flowering by Trehalose-6-Phosphate Signaling in

Arabidopsis thaliana

Vanessa Wahl *et al.*

Science **339**, 704 (2013);

DOI: 10.1126/science.1230406

This copy is for your personal, non-commercial use only.

If you wish to distribute this article to others, you can order high-quality copies for your colleagues, clients, or customers by [clicking here](#).

Permission to republish or repurpose articles or portions of articles can be obtained by following the guidelines [here](#).

The following resources related to this article are available online at www.sciencemag.org (this information is current as of March 14, 2013):

Updated information and services, including high-resolution figures, can be found in the online version of this article at:

<http://www.sciencemag.org/content/339/6120/704.full.html>

Supporting Online Material can be found at:

<http://www.sciencemag.org/content/suppl/2013/02/07/339.6120.704.DC1.html>

A list of selected additional articles on the Science Web sites **related to this article** can be found at:

<http://www.sciencemag.org/content/339/6120/704.full.html#related>

This article **cites 47 articles**, 17 of which can be accessed free:

<http://www.sciencemag.org/content/339/6120/704.full.html#ref-list-1>

This article has been **cited by** 1 articles hosted by HighWire Press; see:

<http://www.sciencemag.org/content/339/6120/704.full.html#related-urls>

This article appears in the following **subject collections**:

Botany

<http://www.sciencemag.org/cgi/collection/botany>

end resection. In contrast, Rif1 does not appear to be required for the ability of 53BP1 to promote an increase in the mobility of dysfunctional telomeres. The intermediate effect of Rif1 on the fusion of dysfunctional telomeres can be explained based on these two observations. The increased resection of dysfunctional telomeres in absence of Rif1 is likely to be responsible for the mild inhibition of NHEJ. However, in the absence of 53BP1, the effect of increased resection is combined with a defect in the induction of the mobility of the dysfunctional telomeres, resulting in a more severe blockade to NHEJ. Similarly, we propose that Rif1 deletion leads to partial rescue of chromosome misrejoining in PARPi/BRCA1 shRNA-treated cells because the control of 5' end resection is only one of multiple mechanisms by which 53BP1 acts. One possibility is that the other mechanism used by 53BP1 in this context, similar to what happens at dysfunctional telomeres, involves the induction of

DSB mobility that increases the chance that DSB misrejoining occurs.

References and Notes

1. A. T. Noon, A. A. Goodarzi, *DNA Repair* **10**, 1071 (2011).
2. I. M. Ward, K. Minn, J. van Deursen, J. Chen, *Mol. Cell. Biol.* **23**, 2556 (2003).
3. J. C. Morales *et al.*, *J. Biol. Chem.* **278**, 14971 (2003).
4. S. Difilippantonio *et al.*, *Nature* **456**, 529 (2008).
5. N. Dimitrova, Y. C. Chen, D. L. Spector, T. de Lange, *Nature* **456**, 524 (2008).
6. S. F. Bunting *et al.*, *Cell* **141**, 243 (2010).
7. A. Bothmer *et al.*, *Mol. Cell* **42**, 319 (2011).
8. A. Sfeir, T. de Lange, *Science* **336**, 593 (2012).
9. L. Xu, E. H. Blackburn, *J. Cell Biol.* **167**, 819 (2004).
10. J. Silverman, H. Takai, S. B. Buonomo, F. Eisenhaber, T. de Lange, *Genes Dev.* **18**, 2108 (2004).
11. M. S. Huen *et al.*, *Mol. Cell* **37**, 854 (2010).
12. C. F. Hardy, L. Sussel, D. Shore, *Genes Dev.* **6**, 801 (1992).
13. S. Anbalagan, D. Bonetti, G. Lucchini, M. P. Longhese, *PLoS Genet.* **7**, e1002024 (2011).
14. D. Bonetti *et al.*, *PLoS Genet.* **6**, e1000966 (2010).
15. S. B. Buonomo, Y. Wu, D. Ferguson, T. de Lange, *J. Cell Biol.* **187**, 385 (2009).
16. D. Cornacchia *et al.*, *EMBO J.* **31**, 3678 (2012).

17. S. Yamazaki *et al.*, *EMBO J.* **31**, 3667 (2012).
18. A. A. Sartori *et al.*, *Nature* **450**, 509 (2007).
19. X. Yu, L. C. Wu, A. M. Bowcock, A. Aronheim, R. Baer, *J. Biol. Chem.* **273**, 25388 (1998).
20. A. K. Wong *et al.*, *Oncogene* **17**, 2279 (1998).
21. H. Takai, A. Smogorzewska, T. de Lange, *Curr. Biol.* **13**, 1549 (2003).

Acknowledgments: We thank D. White for expert mouse husbandry and M. Nussenzweig for providing mutant 53BP1 constructs. M.Z. was supported by a Brno Ph.D. talent fellowship and by a grant from the Czech Science Foundation to Ctirad Hofr (P205/12/0550) (see supplementary materials for detailed acknowledgement). This work was supported by a grant from the Breast Cancer Research Foundation to T.d.L. T.d.L. is an American Cancer Society Research Professor.

Supplementary Materials

www.sciencemag.org/cgi/content/full/science.1231573/DC1
Materials and Methods
Figs. S1 to S4
References (22–28)

16 October 2012; accepted 14 December 2012
Published online 10 January 2013;
10.1126/science.1231573

Regulation of Flowering by Trehalose-6-Phosphate Signaling in *Arabidopsis thaliana*

Vanessa Wahl,^{1*} Jathish Ponnu,² Armin Schlereth,¹ Stéphanie Arrivault,¹ Tobias Langenecker,² Annika Franke,¹ Regina Feil,¹ John E. Lunn,¹ Mark Stitt,¹ Markus Schmid^{2*}

The timing of the induction of flowering determines to a large extent the reproductive success of plants. Plants integrate diverse environmental and endogenous signals to ensure the timely transition from vegetative growth to flowering. Carbohydrates are thought to play a crucial role in the regulation of flowering, and trehalose-6-phosphate (T6P) has been suggested to function as a proxy for carbohydrate status in plants. The loss of *TREHALOSE-6-PHOSPHATE SYNTHASE 1* (*TPS1*) causes *Arabidopsis thaliana* to flower extremely late, even under otherwise inductive environmental conditions. This suggests that *TPS1* is required for the timely initiation of flowering. We show that the T6P pathway affects flowering both in the leaves and at the shoot meristem, and integrate *TPS1* into the existing genetic framework of flowering-time control.

The transition from vegetative to reproductive development is an important phase change in a plant's life. When timed correctly, the transition helps to ensure reproductive success and therefore has adaptive value. For this reason, plants have evolved an intricate genetic network that controls the onset of flowering in response to environmental and endogenous signals such as day length, temperature, hormonal status, and carbohydrate availability (*1*). Day length is perceived in the

leaves, where a sufficiently long day (i.e., an inductive photoperiod) leads to induction of the *FLOWERING LOCUS T* (*FT*) gene (*2–7*). The FT protein functions as a long-distance signal (florigen) that is transported to the shoot meristem, where it interacts with the bZIP transcription factor FD and triggers the formation of flowers (*8–11*).

In contrast to the detailed understanding of the photoperiod pathway, relatively little is known about the contribution of carbohydrates to the regulation of flowering (*12*). Mutations in genes of key enzymes in sugar and starch metabolism such as *HEXOKINASE1* (*HXK1*) and *PHOSPHO-GLUCOMUTASE1* (*PGM1*) have been shown to affect various aspects of development, including flowering (*13*). A particularly striking example in this respect is *TREHALOSE-6-PHOSPHATE SYNTHASE 1* (*TPS1*), which catalyzes the formation of trehalose-6-phosphate (T6P) from

glucose-6-phosphate and uridine diphosphate (UDP)–glucose (*13, 14*). T6P, which is found only in trace amounts in most plants, has been suggested to function as a signaling molecule that relays information about carbohydrate availability to other signaling pathways (*15*). In agreement with the proposed role of T6P as a central hub in carbon signaling, *TPS1* loss-of-function mutants are embryonic lethal (*16*). Expression of *TPS1* from the seed-specific *ABI3* promoter has been shown to be sufficient to rescue the embryo defect, but the resulting homozygous *tps1* *ABI3:TPS1* plants develop slowly and senesce before entering the reproductive phase (*17*). Homozygous *tps1-2* mutants have also been recovered using a chemically inducible rescue construct (*GVG:TPS1*), which enables induction of *TPS1* by dexamethasone application, allowing the *tps1-2* *GVG:TPS1* embryos to be rescued to give viable plants that can be stably maintained (*18*). The resulting *tps1-2* *GVG:TPS1* plants flower extremely late, producing infertile flowers on shoots that simultaneously arise from the shoot apical meristem (SAM) and axillary meristems, or completely fail to flower, even under inductive photoperiod. These findings indicate that *TPS1* plays a critical role in controlling the transition to flowering. However, it is currently unclear where *TPS1* is integrated into the canonical flowering-time pathways.

To better understand the molecular function of *TPS1*, we first confirmed its effect on flowering by knocking down *TPS1* expression with the use of an artificial microRNA (*35S:amiR-TPS1*; figs. S1 and S2) (*19*). This resulted in a significant 25 to 30% reduction in T6P levels (fig. S3) and a delay in flowering by more than 20 leaves (Table 1, experiment 1; fig. S4). In contrast, sucrose levels were significantly higher in *35S:amiR-TPS1* plants (fig. S4), indicating that carbohydrate availability as such was not compromised in those plants. These findings highlight

¹Department of Metabolic Networks, Max Planck Institute of Molecular Plant Physiology, Am Mühlenberg 1, 14476 Potsdam, Germany.

²Department of Molecular Biology, Max Planck Institute for Developmental Biology, Spemannstr. 35, 72076 Tübingen, Germany.

*To whom correspondence should be addressed. E-mail: vanessa.wahl@mpimp-golm.mpg.de (V.W.); maschmid@tuebingen.mpg.de (M.S.)

the importance of TPS1 activity and T6P signaling, jointly referred to as the T6P pathway, in regulating the floral transition.

To investigate whether the T6P pathway integrates into the photoperiod pathway, we next determined the diurnal changes in T6P concentration. We observed a pronounced rhythmicity in

T6P across a 72-hour time course, with maxima in T6P levels toward the end of the day (Fig. 1A), broadly following the previously reported diurnal changes of sucrose levels (15). This is exactly the time of day when the circadian and light-regulated CONSTANS (CO) protein normally induces the expression of *FT* (6, 20, 21).

Expression of *CO* (Fig. 1B) and that of its upstream regulator *GIGANTEA* (*GI*) (fig. S5) were unchanged in the *tps1-2 GVG:TPS1* mutant. In contrast, the induction of *FT* at the end of the long day (LD) was abolished in *tps1-2 GVG:TPS1* plants (Fig. 1C). Similarly, expression of *TWIN SISTER OF FT* (*TSF*), which has been shown to follow the same diurnal regulation and to contribute to the induction of flowering (22), was substantially reduced in *tps1-2 GVG:TPS1* plants at the end of the LD (fig. S5). Expression of *FT* and *TSF* was also substantially reduced in a developmental series in the *35S:amiR-TPS1* line (fig. S6). Furthermore, *FT* expression in *tps1-2 GVG:TPS1* plants could be significantly induced by dexamethasone application (fig. S7), confirming that the T6P pathway is required for *FT* and *TSF* expression under inductive photoperiod.

The finding that *FT* and *TSF* expression is almost completely abolished in the *tps1-2 GVG:TPS1*

Table 1. Flowering times of mutants and transgenic plants. RLN, rosette leaf number; CLN, cauline leaf number; TLN, total leaf number; *n*, number of individuals; #, identifier of individual transgenic line; NA, not applicable.

| | RLN | CLN | TLN | TLN SD | TLN range | <i>n</i> |
|------------------------------------|------|------|-------|--------|-----------|----------|
| Experiment 1 (long days) | | | | | | |
| Col-0 (wild type) | 9.1 | 2.1 | 11.2 | ±1.0 | 9–14 | 20 |
| <i>35S:amiR-TPS1</i> #5 | 27.0 | 6.1 | 33.1 | ±2.3 | 30–36 | 20 |
| <i>35S:amiR-TPS1</i> #6 | 27.9 | 6.5 | 34.4 | ±2.9 | 27–43 | 20 |
| <i>CLV3:TPS1</i> #7 | 2.8 | 1.8 | 4.6 | ±2.1 | 2–9 | 9 |
| <i>CLV3:TPS1</i> #15 | 1.5 | 2.0 | 3.5 | ±0.6 | 3–4 | 4 |
| <i>CLV3:otsB</i> #7 | 14.2 | 3.6 | 17.8 | ±1.4 | 16–20 | 10 |
| <i>CLV3:otsB</i> #9 | 15.0 | 3.9 | 18.9 | ±2.0 | 16–23 | 10 |
| Experiment 2 (long days) | | | | | | |
| Col-0 (wild type) | 10.2 | 1.8 | 12.0 | ±1.1 | 9–13 | 20 |
| <i>ft-10</i> | 38.1 | 8.1 | 46.2 | ±2.1 | 43–50 | 20 |
| <i>35S:amiR-TPS1</i> #5 | 29.9 | 7.3 | 37.2 | ±2.3 | 32–41 | 20 |
| <i>35S:amiR-TPS1</i> #6 | 32.5 | 7.2 | 39.7 | ±2.8 | 35–44 | 20 |
| <i>ft-10 35S:amiR-TPS1</i> #5 | 39.7 | 9.6 | 49.3 | ±1.7 | 46–53 | 20 |
| <i>ft-10 35S:amiR-TPS1</i> #6 | 40.5 | 9.6 | 50.1 | ±1.9 | 47–53 | 20 |
| Experiment 3 (long days) | | | | | | |
| Col-0 (wild type) | 9.0 | 1.3 | 10.3 | ±1.0 | 9–12 | 20 |
| <i>35S:amiR-TPS1</i> #6 | 29.6 | 6.3 | 35.9 | ±1.9 | 33–40 | 19 |
| <i>35S:FT</i> | 3.8 | 1.2 | 5.0 | ±0.4 | 4–6 | 15 |
| <i>SUC2:FT</i> | 3.6 | 1.1 | 4.7 | ±0.5 | 4–5 | 15 |
| <i>35S:FT 35S:amiR-TPS1</i> #6 | 4 | 1.4 | 5.4 | ±0.5 | 5–6 | 20 |
| <i>SUC2:FT 35S:amiR-TPS1</i> #6 | 4.1 | 1.4 | 5.5 | ±0.5 | 5–6 | 20 |
| Experiment 4 (short days) | | | | | | |
| Col-0 (wild type) | 58.9 | 3.1 | 62.0 | ±2.0 | 59–65 | 20 |
| <i>tps1-2 GVG:TPS1</i> | >100 | NA | >100 | NA | >100 | 20 |
| Experiment 5 (short days) | | | | | | |
| Col-0 (wild type) | 54.1 | 9.6 | 63.7 | ±2.5 | 59–69 | 18 |
| <i>CLV3:TPS1</i> #7 | 24.0 | 5.8 | 29.8 | ±2.9 | 23–33 | 21 |
| <i>CLV3:TPS1</i> #15 | 37.4 | 8.8 | 46.2 | ±3.3 | 38–50 | 20 |
| Experiment 6 (long days) | | | | | | |
| Col-0 (wild type) | 8.1 | 2.0 | 10.1 | ±0.6 | 9–11 | 20 |
| <i>ft-10</i> | 37.6 | 7.3 | 44.9 | ±1.9 | 42–48 | 20 |
| <i>CLV3:TPS1</i> #7 | 3.8 | 1.9 | 5.7 | ±0.7 | 5–7 | 18 |
| <i>CLV3:TPS1</i> #7 <i>ft-10</i> | 13.7 | 2.5 | 16.2 | ±1.3 | 15–20 | 20 |
| Experiment 7 (long days) | | | | | | |
| Col-0 (wild type) | 9.0 | 1.8 | 10.8 | ±1.1 | 9–14 | 20 |
| <i>35S:miR156</i> | 29.6 | 4.2 | 33.8 | ±2.6 | 29–38 | 20 |
| <i>35S:amiR-TPS1</i> #5 | 29.5 | 6.8 | 36.3 | ±1.9 | 30–38 | 20 |
| <i>35S:amiR-TPS1</i> #6 | 32.4 | 6.8 | 39.2 | ±2.1 | 36–42 | 20 |
| <i>35S:miR156 35S:amiR-TPS1</i> #5 | >100 | NA | >100 | NA | >100 | 20 |
| <i>35S:miR156 35S:amiR-TPS1</i> #6 | >100 | NA | >100 | NA | >100 | 20 |
| Experiment 8 (short days) | | | | | | |
| Col-0 (wild type) | 57.1 | 10.5 | 67.6 | ±2.2 | 65–72 | 20 |
| <i>35S:miR156</i> | 97.8 | 4.6 | 102.4 | ±3.8 | 97–110 | 20 |
| <i>35S:amiR-TPS1</i> #6 | 56.3 | 8.4 | 64.7 | ±2.6 | 60–69 | 20 |
| <i>35S:miR156 35S:amiR-TPS1</i> #6 | >120 | NA | >120 | NA | >120 | 20 |
| Experiment 9 (long days) | | | | | | |
| Col-0 (wild type) | 10.6 | 2.3 | 12.9 | ±1.7 | 11–17 | 20 |
| <i>tps1-2 GVG:TPS1</i> | >80 | NA | >80 | NA | >80 | 20 |
| <i>35S:MIM156</i> | 2.8 | 4.3 | 7.1 | ±1.0 | 5–9 | 20 |
| <i>35S:MIM156 tps1-2 GVG:TPS1</i> | 8.3 | 3.9 | 12.2 | ±1.2 | 10–14 | 20 |

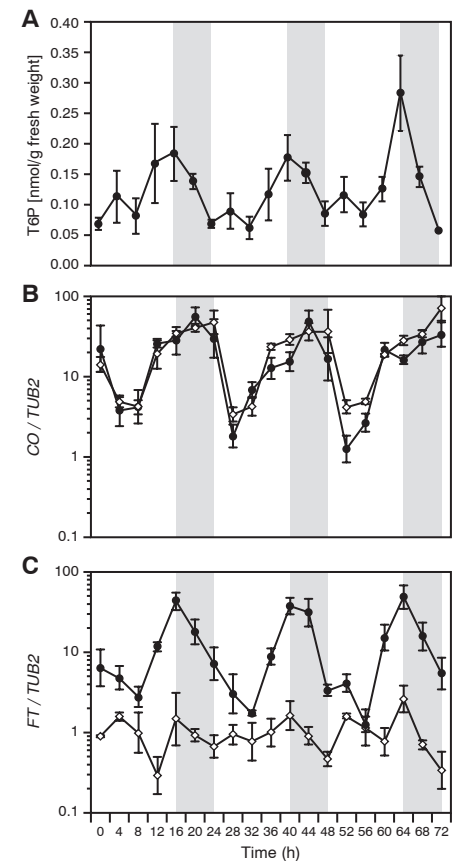


Fig. 1. Diurnal time course of T6P and flowering-time genes over 72 hours. (A) T6P levels in whole 12- to 14-day-old Col-0 rosettes. Error bars indicate SD of the mean. (B and C) Expression of *CO* (B) and *FT* (C) in 12- to 14-day-old Col-0 (solid circles) and *tps1-2 GVG:TPS1* (open diamonds) rosettes. Expression was determined by qRT-PCR using three biological replicates with three technical repetitions each and normalized to *TUB2*. Shaded areas indicate dark periods. Error bars indicate the upper and lower limit of the SD of the mean.

mutant and strongly attenuated in *35S:amiR-TPS1* lines explains, to a large extent, the late flowering of these genotypes. Loss of *FT* function—as, for example, in the strong T-DNA insertion mutant *ft-10*—results in delayed flowering, specifically under LD (supplementary text and table S1). Genetic analyses demonstrated that *ft-10 35S:amiR-TPS1* double mutants flowered only marginally later in LD than did *ft-10* plants (Table 1, experiment 2), indicating that the two genes act in the same pathway. Moreover, expression of *FT* from the constitutive *35S* promoter or the phloem companion cell-specific *SUC2* promoter, which has been shown by several studies to induce flowering independently of photoperiod (supplementary text and table S1), almost completely suppressed the late flowering of *35S:amiR-TPS1* (Table 1, experiment 3), confirming that the T6P pathway acts upstream of *FT* in the photoperiod pathway.

In contrast to *ft-10* mutants, which are late-flowering only under inductive LD conditions, *tps1-2 GVG:TPS1* mutants flowered late irrespective of day length (Table 1, experiment 4). This suggests that the T6P pathway also interferes with other floral signals in addition to the photoperiod pathway, and that it does so in a tissue separate from the leaves where day length is perceived. The most likely tissue for a non-leaf function of the T6P pathway is the SAM, where the different flowering-time pathways converge to regulate the expression of a small set of integrator genes, the expression of which ultimately decides whether the plant will make the transition to flowering (1).

TPS1 expression was detected by RNA in situ hybridization in the flanks of the meristem encircling the center of the SAM (Fig. 2, A to D, and fig. S8). In agreement with a proposed role of the T6P pathway in regulating flowering time at the SAM, T6P levels increased significantly during the transition to flowering in meristems of LD-grown plants (Fig. 2E) as well as in the meristems of plants in which flowering had been induced synchronously by shifting them from short day (SD) to LD (Fig. 2F). In dissected meristems of the latter, we observed a very strong correlation between T6P and sucrose levels (Fig. 2G), highlighting the role of T6P as an indicator of a plant's carbon status not only in vegetative tissues but also in the SAM.

These observations prompted us to express *TPS1* and the T6P-catabolizing enzyme trehalose-6-phosphate phosphatase, encoded by the *otsB* gene from *Escherichia coli*, in the SAM (13). Misexpression of *TPS1* from the stem cell niche-specific *CLV3* promoter (*CLV3:TPS1*) resulted in very early flowering under inductive LD as well as under noninductive SD conditions, whereas expression of *otsB* (*CLV3:otsB*) had the opposite effect (Table 1, experiments 1 and 5; Fig. 2, H to K; fig. S9). We found that the expression of *CLV3:TPS1* was sufficient to almost completely rescue the late flowering of *ft-10* mutants, demonstrating that the T6P pathway can act largely

independently of *FT* to induce flowering at the shoot meristem (Table 1, experiment 6). Taken together, these findings indicate that *TPS1* and T6P signaling are important regulators of the transition to flowering at the SAM.

To identify potential targets of the T6P pathway in the SAM, we performed a microarray analysis of dissected apices of 21-day-old SD-grown vegetative *tps1-2 GVG:TPS1* and wild-type plants (figs. S10 to S12). Transcript levels for genes known to be involved in integrating diverse flowering-time signals at the apex such as photoperiod (fig. S10), ambient temperature, prolonged periods of cold (vernalization) (fig. S11), and gibberellic acid (fig. S12) were unchanged or displayed only minor, statistically insignificant expression changes in the *tps1-2 GVG:TPS1* mutant relative to the wild type. The notable exception was *SQUAMOSA PROMOTER BINDING PROTEIN-LIKE 3* (*SPL3*), a known component of the age pathway of floral induction in *Arabidopsis thaliana* (23–26). Expression of *SPL3* was reduced by 60% in *tps1-2 GVG:TPS1* (Fig. 3E). The reduced expression of *SPL3* in *tps1-2 GVG:TPS1* was verified by quantitative reverse transcription polymerase chain reaction (qRT-PCR) on dissected meristems of 10- to 50-day-old SD-grown plants (Fig. 3F). This analysis also identified two closely related genes—*SPL4* and *SPL5* (23, 26), whose

expression was below the detection limit in the microarray experiment—as potential targets of the T6P pathway at the SAM (Fig. 3, E and F).

SPL genes have been shown to be regulated by diverse flowering signals and to form the molecular output of a pathway that regulates flowering as a function of a plant's age (25). The age-dependent induction of flowering is a fail-safe to ensure that plants eventually flower even in the absence of inductive signals. This is accomplished by the gradual reduction of miR156 levels independently of other signals, and a corresponding increase in miR156-targeted *SPL* transcripts, as plants age (25, 27). We compared mature miR156 levels at the meristem in SD-grown wild-type and *tps1-2 GVG:TPS1* plants at different times between 10 and 50 days after germination. Between 10 and 30 days after germination, the levels of the mature miR156 were consistently higher in the *tps1-2 GVG:TPS1* mutant relative to the wild type (Fig. 3G), which explains the reduced *SPL3*, *SPL4*, and *SPL5* expression observed in *tps1-2 GVG:TPS1* plants at these times (Fig. 3F). However, as the plants aged, miR156 declined to similarly low levels in both genotypes from 40 to 50 days after germination (Fig. 3G). This decrease of miR156 was accompanied by a strong increase of *SPL3*, *SPL4*, and *SPL5* transcript levels in wild-type plants.

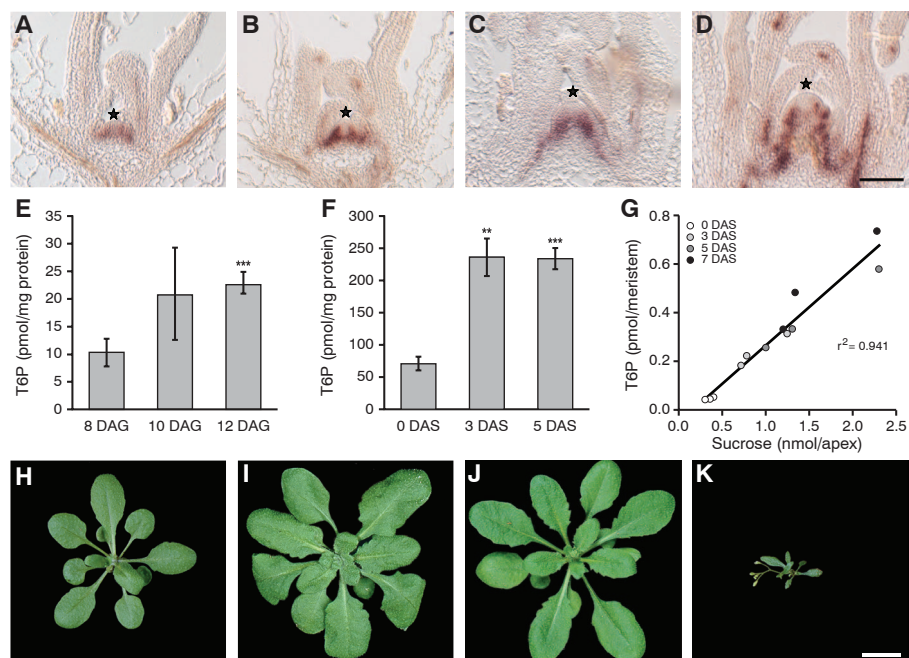


Fig. 2. *TPS1* expression and T6P concentrations in the SAM. (A to D) Detection of *TPS1* expression by RNA in situ hybridization in the SAM in LD-grown plants 6 days after germination (DAG) (A), 8 DAG (B), 10 DAG (C), and 12 DAG (D). Star indicates meristem summit. Scale bar, 100 μ m. (E and F) T6P content in dissected meristems of LD-grown Col-0 plants (E) and 30-day-old SD-grown plants shifted to LD and harvested at 0, 3, and 5 days after the shift (DAS) (F). Error bars denote SD; ** $P < 0.01$, *** $P < 0.001$ (Student's *t* test, based on four biological replicates). (G) Correlation between sucrose and T6P concentration in dissected meristems 0, 3, 5, and 7 days after shift from SD to LD. (H to K) Rosette phenotype of Col-0 (H), *35S:amiR-TPS1* #6 (I), *CLV3:otsB* #9 (J), and *CLV3:TPS1* #7 (K). Scale bar, 1 cm.

In contrast, the increase was strongly attenuated in *tps1-2 GVG:TPS1* plants (Fig. 3G).

Taken together, these results suggest that the T6P pathway controls expression of *SPL3*, *SPL4*, and *SPL5* in the SAM, in part via miR156 and in part independently of the miR156-dependent age pathway. In agreement with these findings, we observed that constitutive expression of miR156, which has been shown by several studies to delay vegetative phase transition and flowering (supplementary text and table S1), combined with down-regulation of *TPS1* (*35S:amiR-TPS1*), had an additive effect on flowering, with the double-transgenic line failing to flower in either LD or SD (Table 1, experiments 7 and 8). In addition, reducing the levels of mature miR156 by the constitutive expression of *MIM156* (28, 29), which sequesters miR156 from its targets, was sufficient to restore flowering in the *tps1-2 GVG:TPS1* mutant (Fig. 3, A to D; Table 1, experiment 9). This provides further evidence that the miR156/age pathway acts at least partially independently of the T6P pathway.

SPL proteins have also been shown to promote *FT* expression in leaves by regulating the expression of two MADS-box transcription factors, *SUPPRESSOR OF OVEREXPRESSION OF CONSTANS 1* (*SOC1*) and *FRUITFUL* (*FUL*) (25, 30). This raised the possibility that the observed repression of *FT* in *tps1-2 GVG:TPS1*

plants (Fig. 1C) was due to reduced expression of *SOC1* and *FUL*. However, expression of these two genes was not changed in the *tps1-2 GVG:TPS1* (fig. S13) and *35S:amiR-TPS1* mutant rosettes (fig. S14) before flowering, which in LD-grown wild-type plants occurs approximately 10 days after germination (fig. S4). These findings suggest that in leaves, the T6P pathway regulates *FT* largely independently of the miR156-SPL module.

Our results demonstrate that the T6P pathway regulates flowering at two sites in the plant (fig. S15). In the leaves, *TPS1* activity is required for the induction of the florigen *FT*, even under inductive photoperiod. This provides a convenient way for the plant to integrate an environmental signal (the activation of *FT* by CO in response to increasing day length in spring) with a physiological signal (the presence of high carbohydrate levels, as indicated by T6P). Together these two inputs ensure that *FT* is expressed when the conditions are optimal—that is, when day length exceeds a certain minimum and the plant has sufficient carbohydrate resources to support the energy-demanding processes of flowering and seed production. In addition, the T6P pathway affects the expression of important flowering-time and flower-patterning genes via the age pathway directly at the SAM independently of the photoperiod pathway. This might

provide a local signal to link developmental decisions in the meristem to the supply of carbohydrates. Thus, the T6P pathway acts as a signal that coordinates the induction of flowering by regulating the expression of key floral integrators in leaves and the SAM.

References and Notes

1. A. Srikanth, M. Schmid, *Cell. Mol. Life Sci.* **68**, 2013 (2011).
2. M. Abe *et al.*, *Science* **309**, 1052 (2005).
3. L. Corbesier, I. Gadisseur, G. Silvestre, A. Jacqmar, G. Bernier, *Plant J.* **9**, 947 (1996).
4. I. Kardalisky *et al.*, *Science* **286**, 1962 (1999).
5. Y. Kobayashi, H. Kaya, K. Goto, M. Iwabuchi, T. Araki, *Science* **286**, 1960 (1999).
6. P. Suárez-López *et al.*, *Nature* **410**, 1116 (2001).
7. P. A. Wigge *et al.*, *Science* **309**, 1056 (2005).
8. L. Corbesier *et al.*, *Science* **316**, 1030 (2007).
9. K. E. Jaeger, P. A. Wigge, *Curr. Biol.* **17**, 1050 (2007).
10. J. Mathieu, N. Warthmann, F. Küttner, M. Schmid, *Curr. Biol.* **17**, 1055 (2007).
11. S. Tamaki, S. Matsuo, H. L. Wong, S. Yokoi, K. Shimamoto, *Science* **316**, 1033 (2007).
12. L. Corbesier, P. Lejeune, G. Bernier, *Planta* **206**, 131 (1998).
13. M. J. Paul, L. F. Primavesi, D. Jhureea, Y. Zhang, *Annu. Rev. Plant Biol.* **59**, 417 (2008).
14. J. Ponnuru, V. Wahl, M. Schmid, *Front. Plant Physiol.* **2**, 70 (2011).
15. J. E. Lunn *et al.*, *Biochem. J.* **397**, 139 (2006).
16. P. J. Eastmond *et al.*, *Plant J.* **29**, 225 (2005).
17. L. D. Gómez, A. Gilday, R. Feil, J. E. Lunn, I. A. Graham, *Plant J.* **64**, 1 (2010).
18. A. J. H. van Dijken, H. Schluepman, S. C. Smeekens, *Plant Physiol.* **135**, 969 (2004).
19. See supplementary materials on Science Online.
20. T. Imaizumi, T. F. Schultz, F. G. Harmon, L. A. Ho, S. A. Kay, *Science* **309**, 293 (2005).
21. F. Valverde *et al.*, *Science* **303**, 1003 (2004).
22. A. Yamaguchi, Y. Kobayashi, K. Goto, M. Abe, T. Araki, *Plant Cell Physiol.* **46**, 1175 (2005).
23. G. Cardon *et al.*, *Gene* **237**, 91 (1999).
24. G. H. Cardon, S. Höhmann, K. Nettessheim, H. Saedler, P. Huijser, *Plant J.* **12**, 367 (1997).
25. J. W. Wang, B. Czech, D. Weigel, *Cell* **138**, 738 (2009).
26. Z. Yang *et al.*, *Gene* **407**, 1 (2008).
27. G. Wu *et al.*, *Cell* **138**, 750 (2009).
28. J. M. Franco-Zorrilla *et al.*, *Nat. Genet.* **39**, 1033 (2007).
29. M. Todesco, I. Rubio-Somoza, J. Paz-Ares, D. Weigel, *PLoS Genet.* **6**, e1001031 (2010).
30. A. Yamaguchi *et al.*, *Dev. Cell* **17**, 268 (2009).

Acknowledgments: We thank C. Abel and J. Olas for help with plant work, and U. Krause for assistance with sample collection. The *tps1-2 GVG:TPS1* mutant was obtained from the Smeekens laboratory, University of Utrecht, Netherlands. Microarray data reported in this study have been deposited with EBI ArrayExpress (E-MEXP-3727). Supported by Deutsche Forschungsgemeinschaft grant SCHM-1560/6 and Priority Program 1530 (SPP1530) grant SCHM-1560/8 (M.S.), European Commission FP7 collaborative project TiMet contract 245143 (M.St.), and the Max Planck Society. The authors declare no conflict of interest.

Supplementary Materials

www.sciencemag.org/cgi/content/full/339/6120/704/DC1
Materials and Methods
Supplementary Text
Figs. S1 to S15
Tables S1 and S2
References (31–49)

18 September 2012; accepted 3 December 2012
10.1126/science.1230406

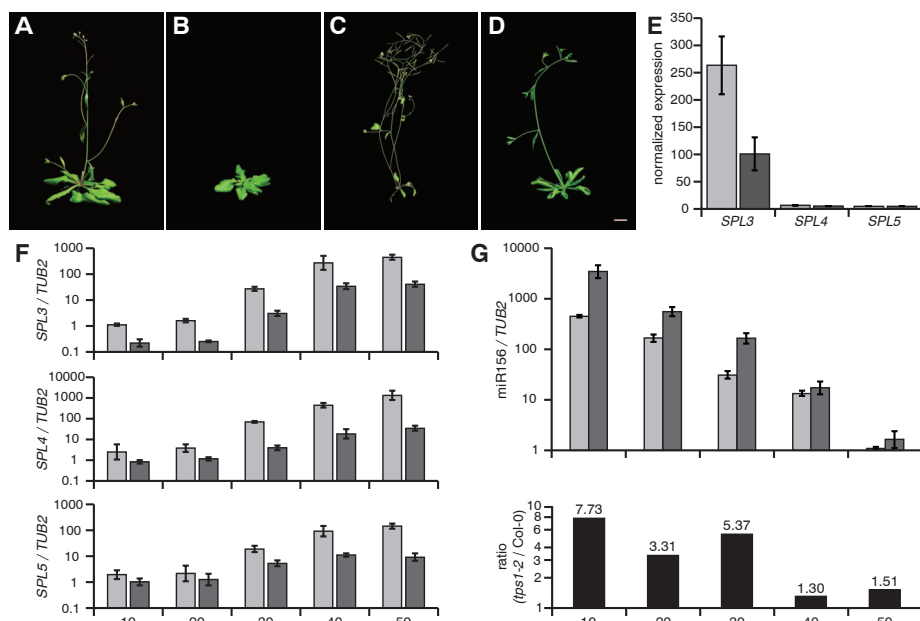


Fig. 3. SPL/miR156 module and T6P signaling. (A to D) Flowering-time phenotypes of Col-0 (A), *tps1-2 GVG:TPS1* (B), *35S:MIM156* (C), and homozygous *tps1-2 GVG:TPS1 35S:MIM156* (D) plants. Scale bar, 1 cm. (E) Expression of *SPL3*, *SPL4*, and *SPL5* in apices of 21-day-old SD-grown Col-0 (light gray) and *tps1-2 GVG:TPS1* (dark gray) as determined by microarray hybridization. Error bars indicate minimum and maximum values of two biological replicates. (F) Expression of *SPL3*, *SPL4*, and *SPL5* in SD-grown Col-0 (light gray) and *tps1-2 GVG:TPS1* (dark gray) plants 10, 20, 30, 40, and 50 days after germination. (G) Relative levels of mature miR156 as measured by qRT-PCR in apices of SD-grown Col-0 (light gray) and *tps1-2 GVG:TPS1* (dark gray) plants 10, 20, 30, 40, and 50 days after germination. Error bars in (F) and (G) denote upper and lower limit of SD of three biological replicates with three technical repetitions each.